Formation of metamorphic core complexes in non-over-thickened continental crust: A case study of Liaodong Peninsula (East Asia)

Kun Wang, Evguenii Burov, Charles Gumiaux, Yan Chen, Gang Lu, Leila Mezri, Liang Zhao

HAL Id: insu-01225346

https://insu.hal.science/insu-01225346

Submitted on 6 Nov 2015
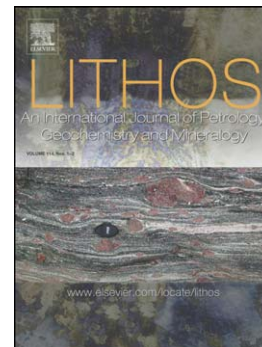
Accepted Manuscript

Formation of Metamorphic Core Complexes in non-over-thickened continental crust: A case study of Liaodong Peninsula (East Asia)

Kun Wang, Evgueni Burov, Charles Gumiaux, Yan Chen, Gang Lu, Leila Mezri, Liang Zhao

Formation of Metamorphic Core Complexes in non-over-thickened continental crust:

A case study of Liaodong Peninsula (East Asia)

Kun Wang[1,2,3,*], Evgueni Burov[2,3], Charles Gumiaux[4,5,6], Yan Chen[4,5,6], Gang Lu[1], Leila Mezri[2,3],Liang Zhao [1,*]

[1] *State Key Laboratory of Lithospheric Evolution, Institute of Geology and Geophysics, Chinese Academy of Sciences, Beijing, China*

[2]*Sorbonne Universités, UPMC Univ Paris 06, UMR 7193, Institut des Sciences de la Terre Paris (iSTeP), F-75005 Paris, France*

[3]*CNRS, UMR 7193, Institut des Sciences de la Terre Paris (iSTeP), F-75005 Paris, France*

[4]*Université d'Orléans, ISTO, UMR 7327, 45071 Orléans, France*

[5]*CNRS/INSU, ISTO, UMR 7327, 45071 Orléans, France*

[6]*BRGM, ISTO, UMR 7327, BP 36009, 45060 Orléans, France*

[*]Corresponding authors:

Kun Wang (wangkun@mail.iggcas.ac.cn) and Liang Zhao (zhaoliang@mail.iggcas.ac.cn), Institute of Geology and Geophysics, Chinese Academy of Sciences, Beijing, China. Tel: +86-10-82998430.

Abstract

Pre-thickened hot orogenic crust is often considered a necessary condition for the formation of continental metamorphic core complexes (MCCs). However, the discovery of MCCs in the Liaodong

Peninsula, where the crust has a normal thickness (~35 km), challenges the universality of this scenario. Therefore, we implement a series of 2-D numerical thermo-mechanical modeling experiments in which we investigate the conditions of MCC formation in normal crusts, as well as the relationships between the underlying mechanisms and the syn-rift basin evolution. In these experiments, we explore the impact of the lithostratigraphic and thermo-rheological structure of the crust. We also examine the lithosphere thickness, strain softening, extension rate and surface erosion/ sedimentation processes. The experiments demonstrate that high thermal gradients and crustal heterogeneities result only in a symmetric spreading dome, which is geometrically incompatible with the observations of the MCCs in the Liaodong Peninsula. According to our further findings, the strain softening should play a key role in the development of asymmetric strain localization and domal topography uplift, while synchronous surface erosion controls the polarity of the syn-rift basin. The synthetic model data are compatible with the geological observations and cooling history based on the thermo-chronology for the eastern part of the East Asia during the late Mesozoic to the early Cenozoic. The model-predicted P-T-t paths are essentially different from those inferred for the other known MCCs, confirming the exceptional character of the MCC formation in the wide rift system of the East Asia.

1. Introduction

The concept of the Metamorphic Core Complex (MCC) was introduced during the late 1970s based on tectonic surveys in the Basin and Range Province (USA) (Coney, 1974; Coney and Harms, 1984; Davis and Coney, 1979; Proffett, 1977). MCCs develop in extensional settings characterized

by significant amounts of crustal stretching and are regarded as distinctive structures, different from those associated with, for example, wide or narrow rifting (e.g., Buck, 1991). A typical MCC comprises the following: (1) a lower unit of metamorphic and/or plutonic rock exhumed from the lower crust into the upper crust; (2) a shallow unit of upper crustal rocks that do not undergo any metamorphic changes during extension; (3) a detachment structure localized between the lower and upper crustal units that corresponds to a shallow dipping and strongly sheared mylonitic zone, which absorbs much of the movement during the exhumation of the lower crust rocks; and (4) differently from "usual" rifts, the Moho below an MCC is nearly horizontal or only slightly uplifted(Buck, 1991; Coney and Harms, 1984; Davis and Coney, 1979; Lister and Davis, 1989; Wernicke, 1981). The upper units behave as brittle blocks and experience rather limited stretching during extension. High-angle normal faults rooted in the detachment typically develop within these domains, and their dynamics largely condition the deposition of sediments into the half graben structures. The lower units, having low viscosity and flowing from the lower to upper crustal levels, display penetrative ductile deformation with foliations during extension. A dome is underlined by the bended shape of foliation envelope within the lower crust where carries imprints of the extensional shear zone localized along the detachment and on top of the dome.

Some well-known MCCs have been identified in the Aegean Sea domain (Gautier et al., 1990; Gautier et al., 1993; Jolivet et al., 2013; Lister, 1984), West Antarctica (Richard et al., 1994), East Asia (Li, 2000; Wang et al., 1998; Wu et al., 2000; Wu et al., 2005a; Wu et al., 2005b; Wu et al., 2007), the Norwegian Caledonides (Steltenpohl et al., 2004) and Iran (Verdel et al., 2007). A particular appellation of "Cordilleran style metamorphic core complexes" (Lister, 1984; Liu et al., 2005; Verdel et al., 2007) is also widely applied to metamorphic features of the Cordilleran realm,

although the related kinematic and thermo-mechanical conditions are not completely identical to those associated with the description of the conventional MCC. A remarkably common feature of most of the described MCCs is that they form in orogenically pre-thickened crust (crustal thickness >50 km, Moho temperatures >800°C) (Buck, 1991; Tirel et al., 2008). This observation is therefore often treated as a crucial condition for the formation of MCCs, either during post-orogenic extensional collapse (North American Cordillera) (Foster and Raza, 2002; Gebelin et al., 2011; Mulch et al., 2007) or in back-arc extension settings during ongoing plate convergence (Aegean Sea) (Jolivet and Faccenna, 2000). MCC domes have also been identified in East Asia (EA) in relation to the large-scale continental extension that took place during Mesozoic times. There are strong debates about the thickness of the continental crust before extension in the East Asia. Previous shortening event is argued to drive the extension (Liu et al., 2005; Wang et al., 2011). However, the Songliao basin can provide direct evidence for the crustal thickness in Liaodong Peninsular before MCC exhumation from the shape of faults and the sequential cross-section restoration (Ge et al., 2012). While the major features and kinematics of these structures perfectly correspond to the canonical features of MCCs, no high-pressure metamorphism and no trace of the pre-existing crustal thickening or of a suture zone have been reported in the north eastern part of China (Charles, 2010; Gumiaux et al., 2012). Indeed, the latest event responsible for crustal thickening happened at the boundary between the North China Craton (NCC) and the South China block (SCB) during the Triassic, which represents a nearly 100-Ma time lag with the Meso-Cretaceous extension episode. It is therefore unreasonable to relate the MCC formation in the Liaodong Peninsula (EA) to this post-orogenic extension (Lin et al., 2013a). This atypical tectonic context of the MCCs in the Liaodong Peninsula raises the new question of whether it is possible for an MCC to develop in

4

non-thickened continental crust.

Many analog and numerical experiments have been performed to understand the mechanisms of MCC formation, addressing a number of key conditions leading to MCC development (Brun, 1999; Burov et al., 2014; Huet et al., 2011a; Huet et al., 2011b; Lavier et al., 1999; Tirel et al., 2008; Tirel et al., 2013). Strain localization and weakening (Buck, 1993; Gessner et al., 2007; Lavier et al., 1999), a pre-existing density and/or weak rheological/compositional heterogeneities in the lower crust (e.g.,Brun, 1999; Brun and Sokoutis, 2007; Burov et al., 1994; Petit et al., 1997) are thought to be essential for rift localization and, in particular, for MCC formation (Brun, 1999; Brun and Sokoutis, 2007; Tirel et al., 2008). Later experiments that have tested the impact of the depth, length and position of the compositional heterogeneity (Tirel et al., 2008) showed, however, that the presence of compositional heterogeneities is not essential for the occurrence of a MCC. The extensive parametric study by Tirel et al. (2008) demonstrated that in the case of an orogenic crust with a commonly inferred rheological structure, three conditions should be satisfied: (1) the initial temperature of the Moho must be greater than 800°C, (2) the crustal thickness must be greater than 45 km, and (3) the initial effective viscosities of the lower crust and the underlying mantle should be lower than 10^{20}Pa and 10^{22} Pa, respectively. Rey et al. (2009) additionally demonstrated that the extension rate partitioning (with respect to the rift axis) may have a major effect on the asymmetry of the crustal detachment faults that characterize most MCCs. Thermal gradients due to collisional thermal heritage or asthenospheric heat sources are also considered in some of the previous studies showing the non-negligible impact on the P-T-t paths of the exhumed metamorphic material (Schenker et al., 2012). Even if the initial thermal gradient remains a first-order parameter for structural heritage, the rheological structure might strongly influence the conditions of MCC

development. Huet et al. (2011a, 2011b) showed, in particular, that an unusual "inverted" rheological structure resulting from orogenic nappe stacking may result in acceleration of the growth rate of the extensional instabilities, enabling MCC formation even in relatively cold crust (Moho temperature ~600°C–700°C). Finally, Tirel et al. (2013) developed a model where MCC forms as a result of stacking and exhumation of continental terrains in a back-arc extension context. Moreover, 3D models testing the impact of kinematic extensional boundary conditions demonstrate geometrical disparities between the extensional and transgressive domes, yet without major modifications in the mechanisms of formation of the detachment fault systems (Le Pourhiet et al., 2012). It is still noteworthy, however, that all previous mechanical and thermo-mechanical experiments are based on a common implicit assumption that the MCCs form as a result of the extensional collapse of a thickened crust, either in a post-orogenic intracontinental context or within the framework of subduction-driven burial and back-arc exhumation of crustal units (Tirel et al., 2013). Most of these studies were enlightened by the Aegean Sea either with thickened crust or fast extension rate. None of these geological settings directly correspond to the case of the Liaodong Peninsula.

In this study, we therefore examine the particular conditions for the thermal and mechanical evolution of MCCs in "normal" crustal thickness settings. With this goal, we implement a series of 2D thermo-mechanical numerical experiments assuming a normal 35-km-thick crust. We further try to elucidate some additional key factors of MCC formation, such as the extension rate, initial thermal gradient, strain softening, erosion/sedimentary rates, initial litho-rheological stratification of the crust, and lithospheric thickness. Finally, after incorporating all available geological and geophysical data, the models are applied to the natural case of the Liaodong Peninsula.

2. Geological Settings

2.1 The wide rift system of the East Asia

East Asia mainly comprises the Central Asian Orogenic Belt (CAOB), the North China Craton (NCC) and the South China Block (Figure 1a) (Charles et al., 2012; Wang et al., 2011). The NCC is an old and relatively small craton dated to approximately 1.85 Ga (Zhao et al., 2001) that locates in-between the CAOB and the SCB bordered by the Permain Solonker Suture Zone (Xiao et al., 2003; Yin and Nie, 1996) and Triassic Qinling-Dabie Orogen (Mattauer et al., 1985) separately. After the final amalgamation of these three tectonic units, the whole tectonic collage experienced an intensive reactivation. A pervasive extension event occurred over ~1500km wide from South China up to the Baikal Lake. The geological features associated with the extension are characterised by the opening of large-scaled extensional basins and the emplacement of numerous plutonic and volcanic massifs in East Mongolia and East China (Figure 1a). Mesozoic Sedimentation is characterized by graben or half graben such as in the region of Songliao, Yingen, Erlian, Hailar and East Gobi (Graham et al., 2001; Meng, 2003; Ren et al., 2002). For the rather large intracontinental Songliao basin (~260 000 km^2), both paleontological (Li, 2001) and radiochronological (Chen et al., 1999; Wang et al., 2002) dating show that its opening began in the Late Jurassic in the north and progressed southwards until the latest Cretaceous. Several intensively deformed metamorphic domes and associated granitic intrusions underlying a large extensional shear zone have been identified during late Mesozoic, including Buteel and Zagan (South Lake Baikal, Donskaya et al., 2008; Sklyarov et al., 1997), Yagan-Onch Hayrhan (Southern CAOB, Webb et al., 1999), Hohhot, Louzidian and Yumengshan (Northern NCC, Darby et al., 2001; Davis and Zheng, 1988; Wang et al., 2002; Wang et al., 2004) Linglong (Jiaodong Peninsula, Charles et al., 2011a, b), Yiwulüshan, Liaonan and Gudaoling

7

(Liaodong Peninsula, Charles et al., 2012; Lin et al., 2013a, b; Liu et al., 2005; Xu et al., 1994), Beidabie and Xiaoqinling (Qinling-Dabie Orogen, Wang et al., 1998; Zhang et al., 1997), Lushan and Hongzhen (South China, Zhu et al., 2010; Lin et al., 2000) MCCs. All these MCCs record common NW-SE crustal stretching, and they satisfy all the above-mentioned conditions to join the Cordilleran-type MCC's family. Coincident with the formation of MCC, the Yanshanian tectono-magmatic activity occurred with a peak period at around ~120-130Ma in eastern and north eastern China (Wang et al., 2006). Numerous I-, A-type and alkaline granitic and plutonic rocks, breccia pipes, felsic and alkali basaltic lavas occupy large areas of the EA (Wang et al., 1998; Wu et al., 2005a; Wu et al., 2005b), emphasizing the possibility of lithospheric weakening. With all features involved so far, a wide rift system is an incontrovertible fact in East Asia during Late Mesozoic. Also noteworthy is that the NCC coevally experienced enigmatic cratonic deconstruction. It has been proposed that the eastern part of the NCC experienced significant lithospheric thinning during the Mesozoic to Cenozoic (Wu et al., 2005a; Wu et al., 2005b; Zhu et al., 2012), from a thick (~200 km) Archean or Paleoproterozoic lithosphere to a current thickness of only ~80 km (Chen et al., 2006; Chen et al., 2008; Griffin et al., 1998; Menzies et al., 1993). High-resolution seismic tomography and shear wave splitting data (Zhao et al., 2009; Zhao et al., 2012; Zhao et al., 2013) suggest that interactions between the cratonic lithosphere and the underlying mantle flow have played an important role in the evolution of the NCC and likely linked to the Paleo-Pacific subduction.

2.2 Crustal thickness and thermal structure of the lithosphere

The Liaodong Peninsula is located in the north eastern part of China off the north coast of Bohai Bay and Songliao basin, where massive regional work has been launched since twenty century. Receiver function studies and deep seismic sounding data show an East-West trend in crustal

thinning, with the Moho depth reduced from ~40 km in the western part of the NCC to ~28-32 km around the Bohai Bay (Hao et al., 2007; Li et al., 2006; Wei et al., 2012; Zheng et al., 2008; Zheng et al., 2009). Recently, Ge et al. (2012) inferred a two-stage scenario of extension based on a sequential restoration of lithospheric cross-sections derived from 2D seismic and borehole data across the region of the Songliao basin (Figure 1b). Most of the Sonliao basin sits on the CAOB, whereas the southernmost part is on the northern margin of the NCC and close to the Liaodong Peninsula (Figure 1). Although Songliao Basin spatially belongs to the CAOB from the tectonic frame's point of view, but its rifting episode (130-ca. 102 Ma) is temporally consistent with the development of MCCs in the north eastern NCC. Crustal thickness before and after the two-stage rifting episode are estimated at 50-30 km. In particular, the crustal thickness and average strain rate are approximately 35 km and $0.85*10^{-16}$ s^{-1}, respectively, at the beginning of the second stage of rifting. At this stage, crustal deformation is characterized by localized faulting relevant to the detachment zones that coincide with the exhumation of adjacent MCCs. This work, therefore, provides direct evidence linking the initial crust thickness before the exhumation of the MCC in Liaodong Peninsula. The geothermal history suggests a thermal lithosphere thickness of only ~65-70 km, as supported by vitrinite reflectance studies, which document an exceptional high paleo-surface heat flow (>80 mW/m^2) during late Mesozoic to early Cenozoic times (Fu et al., 2005; Hu et al., 2000; Zhai et al., 2004).

2.3 Deformation of core complexes

Several Cretaceous MCCs are reported here such as Liaonan MCC and Yiwulushan MCC that exhibit NW-SE extensional event in Liaodong Peninsula. However, the early Triassic northward back-thrusting developed in Liaodong peninsular that likely related to the Triassic Sulu orogenic belt

may connect to the final stage of the intracontinental collision between the North China and South China Blocks (Lin et al., 2007). Post-orogenic collapse is therefore sought-after mechanism for extension. It is worth noting that the transition from contraction to extension may not last up to 100Ma while maintaining over-thickened crust (Lin et al., 2013). UHP metamorphic units (dated at 220-210 Ma) are only recognised in the Dabieshan (e.g., Cong, 1996; Faure et al., 2003 and references therein). This tectono-metamorphic event is clearly far older than the late Mesozoic history and far away from Liaodong Peninsular, and therefore, it excludes itself from the rank of post-collisional extension with thickened crust.

The Yiwulüshan massif (Figure 1c) is an extensional structure separated from the Fuxin-Yixian basin by a well-developed detachment zone to the west and by the localised Xia–Liaohe Depression to the east. The Yiwulüshan massif is made of metamorphic and granitic rocks, mostly occupied by weakly or non-foliated Jurassic (160.4±1.8 Ma) granitoid plutons in the central part. Xenoliths of orthogneiss and amphibolites lying between the pluton and country rocks exhibit a NW-SE-oriented foliation. The western deformed border of the dome exhibits a low-angle ductile shear zone that is composed of strongly mylonitized rocks, formed at ~126 Ma according to geochronological constraints.

Similarly, the Liaonan Massif is associated with strong NW–SE horizontal crustal stretching (Figure 1d). Geometrical analysis infers an elliptical core (Lin et al., 2013a; Ren et al., 2002) that consists of Archean metamorphic rocks and Jurassic to Cretaceous granitoids exhibited along the Jinzhou detachment and surrounded by the weakly deformed Neoproterozoic, Paleozoic and Cretaceous upper plate (Liu et al., 2005). Volcanic rocks are recorded in the base of the small Cretaceous half-graben (LBGMR, 1994). Emplacement of syntectonic plutons took place at ca.

130–120 Ma, which is prior to the development of a mylonitic and gneissic sequence, marking the last increments of movement along the detachment, with cooling ages dated at 120–110 Ma.

3. Numerical Model

We used a fully coupled numerical thermo-mechanical modelling approach to investigate the different conditions allowing for the formation of MCCs in non-over-thickened continental crust. The numerical code implemented in this study is FLAMAR-v12 (e.g. Burov and Cloetingh, 2010; Toussaint et al., 2004; Yamato et al., 2009;Appendix in supplementary material), which has been widely used in numerous previous studies of extensional systems and MCC formation (Burov, 2007; Burov and Poliakov, 2001, 2003; Huet et al., 2011a; Huet et al., 2011b; Le Pourhiet et al., 2004; Tirel et al., 2004; Tirel et al., 2008; Tirel et al., 2013; Watremez et al., 2013). The code accounts for elastic-brittle-ductile rheologies and implements passive-markers and dynamic remeshing to handle large strains and displacements (Yamato et al., 2007). Passive markers also allow for tracing the cooling rates and P-T paths.

The 2-D model box (Figure 2, Table 1, Appendix) has a homogeneous spatial grid resolution of 1 km and is 200 km wide, with vertically stratified 35-km-thick normal crust (in supplementary experiments, we also tested models with a 0.5-km spatial resolution and a width up to 500 km to ensure the results are not crucially affected by grid resolution and model width). The mechanical boundary conditions correspond to those used in the previous MCC studies (Huet et al., 2011a; Huet et al., 2011b; Tirel et al., 2008) and correspond to a unilateral extension velocity applied at the right lateral boundary (the left boundary is fixed). The upper boundary condition corresponds to a free surface, and the lower boundary is represented by a Winkler basement that corresponds to a

hydrostatic pliable interface that deflects proportionally to the density contrast between the lithosphere and the underlying asthenosphere (Burov and Poliakov, 2001). The modelled continental crust has a density of 2800 kg/m^3, while the mantle lithosphere density is 3300 kg/m^3.

The initial thermal state of the lithosphere is defined from an unstationary plate cooling model with internal radioactive heat production (e.g. Burov and Diament, 1995 andAppendix in supplementary material). In this study, only 'hot' lithosphere structures are taken into consideration. Therefore, we vary the initially high surface heat flux values (q_0 = 75, 80 and 85mW/m^2) to compute the initial geotherm. These conditions yield elevated initial temperatures at Moho depths (T_m) of 767°C, 837°C and 907°C, respectively (Figure 2). The thermal bottom of the lithosphere is initially set at 1330°C, while the thermal gradient below the lithosphere is adiabatic (e.g. Burov, 2011). The surface temperature is kept at 0°C. The lateral thermal boundary conditions correspond to zero heat outflux.

Because most MCCs exhibit partial melting at the occurrence of rheologically weak migmatites and granitic plutons, two contrasting rheological parameter sets of the lower crust are adopted (Table 1): one represents the commonly inferred crustal rheology and is used for homogeneous crust; the other is used for rheologically weak units and corresponds to rheological properties of wet diorite, which implies a one-order lower effective viscosity than the crust (Figure 2b). A density anomaly is introduced in the lower crust and represents an intrusion of magmatic rocks that are widely observed in NCC.

4. Results

4.1 Predicted rifting modes

We have implemented a detailed experimental numerical study of crustal deformation and evolution under different assumptions on rheological stratification, thermal structure and boundary velocities. Focusing on the impact of a "hot Moho" (in terms of the conventional rift classification by R. Buck (1991)), we subdivided the rifting styles reproduced in our experiments into two types: (1) wide rifting, the dominant mode observed in the case of homogeneous crust, and (2) core complexes, formed in the case of higher thermal gradients (Moho temperature>800°C), slow extension rates (<1cm/y) and stratified crust with rheologically weak lower crust. Figure 3 shows variations in extension dynamics and topography for homogeneous and stratified models, for a unilateral extension rate of 0.33 cm/yr.

In the experiments with quartz-diorite homogeneous crust (yielding a two-layer yield strength envelope, Figure 2b), the mechanical strength of the lithosphere is mainly concentrated in the crust. During the early stages, brittle deformation results in the formation of several faults (Figures 3b and 3d) and then leads to the appearance of symmetrical half-grabens at the upper crustal scale (Figure 3f). The final width of the extended lithosphere reaches to ~270 km (~34% stretching). Crustal and mantle lithospheric thinning is simultaneous and is roughly equivalent. No dome forms in this situation, although a small density anomaly produces some vertical motion of the lower crust, and the resulting surface deformation exhibits deep depression (Figure 3f). Doming does not occur in any of the experiments with a normal homogeneous crust. It is also noteworthy that, throughout the entire extension process, the accumulated shear strain is rather low, even in the vicinity of the Moho boundary, and the overall rifting style corresponds to a wide rifting mode.

Figures 3g-3l illustrate the next set of the experiments, with stratified crustal rheology, where two-stage MCC development occurs following the same evolution pattern as described in Tirel et al.

13

(2004): (1) an "upper crustal necking" phase and (2) a "dome amplification" phase. In these model settings, higher temperatures of the Moho (i.e., higher geothermal gradient) contribute to the low initial viscosity of the lower crust (10^{19}Pa·s) and result in decoupling from the upper crust and mantle lithosphere (Figure 2c). Accordingly, horizontal ductile flow becomes dominant in this scenario. The overall structure shows a lower crust progressively arching upward until it pierces the overlying upper crustal layer, creating a ductile dome. At 4.8 Ma, dominant strain localization (Figure 4a) occurs above the compositional anomaly and thus gives rise to two localized surface uplifts inside the main basin. The experiments with high thermal gradient (907°C at the Moho) produced the expected flat Moho surface (with an inclination of <10°) (Tirel et al., 2008). This naturally requires large-scale ductile flow to feed the exhuming metamorphic dome. However, unlike in the model of Tirel et al. (2008), where the ductile flow is characterized by progressive unilateral channel flow, our models always show relatively symmetrical flows converging from both sides of the lower crust (Figure 4b). Two prominent shear bands format each flank of the surface depression and migrate apart with the amplifying dome. For lower thermal gradients, strong necking at the Moho level occurring during the earlier phases of extension prevents its flattening at later stages.

4.2 Formation of asymmetric MCCs

In all of the experiments described above, a dome can occur if the lower crust is weak. However, there is no asymmetric detachment zone localized along one dome limb. It is widely demonstrated that asymmetric structures are favoured by strain softening (Huismans and Beaumont, 2003; Huismans et al., 2005; Lavier and Buck, 2002) that may be produced by phase changes and by fluids and melts pumped by shear bands. In particular, Scherker et al. (2012) argued, by integrating the different patterns of brittle strain softening, that MCCs can even develop within "cold Moho"

settings and with small initial crustal thickness. We have therefore performed additional experiments in which we have incorporated a brittle strain-softening mechanism. We used a common strain softening scheme with a progressive linear reduction of friction angle from 30° to 5° (Figure 4g) and of cohesion from 20 MPa to 0 (Figure 4h) over the strain range of 0 to 2.The other parameters are identical to the model with a stratified crust and an initial Moho temperature of $T_m=907°C$.

A model with a 0.33-cm/y extension rate depicts a rapid transformation from the initial cross-conjugated fault pattern to asymmetric strain localization (Figures 4c-e). An apparent preferential limb of the conjugate fault dominates the asymmetric crustal necking due to the strain-dependent strength reduction, and consequently the surface undergoes asymmetric uplift. Therefore, the introduction of strain softening results in brittle-ductile transitions within an initially ductile shear zone. With further extension, the shear zone gradually rotates in an anticlockwise direction and accommodates viscous channel flow from the ductile crust.

Expectedly (e.g. Huismans et al., 2005), in the case of a faster rifting rate, relatively symmetric brittle deformation occurs. However, because the boundary velocity partitioning is asymmetric in the models, faster extension also promotes heat advection and hence accelerates the symmetric lateral migration of ductile material as well as the exhumation rate, which induces a preliminary narrow dome with strong relief (Figure 4f). In contrast, a slow extension rate enhances lower crustal flow, resulting in enhanced dome development. This asymmetric evolution stems from a strain-rate-dependent brittle-ductile lithospheric strength where fast far-field extension favours brittle behaviour, while slow extension favours ductile deformation and gravitational instabilities (e.g. Huismans and Beaumont, 2003).

4.3 Relationships between the dome and syn-rift basins

The experiments predict that a supradetachment basin forms simultaneously with the exhumation of metamorphic rocks and accounts for a considerable part of the hanging wall dynamics. These results are incompatible with the observations, although it must be kept in mind that the temporal and spatial relations between the dome and coeval basins are poorly constrained. It is reasonable to suggest that both the formation of the supradetachment basin and the exhumation style and rates may be significantly affected by syn-rift erosion and sedimentation. Therefore, to explore the effect of syn-extensional erosion and deposition, we implemented a surface erosion/sedimentation model based on a diffusion equation (see Appendix in supplementary material). The experiments show that because the erosion rate is higher in the areas of active topography, two elevated flanks at the sides of the basin (e.g., Figure 4e) undergo faster erosion and produce sufficient amounts of sedimentary matter that progressively fill the adjacent depressions. During the crustal 'necking' stage, the major asymmetric syn-rift basin (B1 ~50 km) is located above the rifting neck and is slightly offset with respect to the localized shear zone (Figure 5a). Several shallow (1 km) basins/grabens of different size develop at both sides of the major depression and eventually join each other during the extension. At a later stage, during the 'dome amplification' phase (Figure 5b), the exhumation of the ductile lower crust continues, and a third locus of uplift emerges and splits the initially continuous basin onto two sub-basins. Zone B2l (Figures 5a, b) remains in place, with a stagnation of subsidence characterized by an invariant width and depth of the basin (dashed black line in Figures 5c, e). Zone B2r (Figures 5a, b) is active and migrates to the right and is subject to the upwarp and counter clockwise rotation of the dominant detachment, followed by continuous deepening (solid black line in Figure 5e). Flow in the lower crust may inhibit both lateral deposition and crustal thinning, thus highlighting the importance of coupling between surface processes and the response of ductile flow

16

in the lower crust.

The effect of the surface erosion/sedimentation rate is illustrated in Figures 5c and 5e. The size of the basin steadily evolves with the increasing diffusion coefficient. During the first stage, a wider basin is favoured by a higher erosion rate because the rapid denudation of the elevated flanks broadens the scope of necking and contributes to the necessary increase in the amount of sediment (Figure 5c). However, rapid erosional unloading does not have a strongly negative impact on lower crustal flow, as the ductile lower crust separates the broad basin into two sub-basins at a similar depth (~2500 ± 500 m, the shadow part in Figure 5e) and eventually pulls them apart at similar points in time (~13 ±1 My, shadow part in Figure 5c). In contrast, during the second stage, the asymmetric distribution of the basin vanishes while greatly increasing the erosion rate (e.g. 1000 m^2/y), as shown in Figure 5c, 5e, where the difference of the size (Width × Depth) between the two sub-basins lessens gradually.

Figures 5d and 5f further illustrate the impact of the extension rate on the surface processes. The filling of the basin requires supply of the eroded matter from both vertical and horizontal directions. If the extension is rapid, horizontal widening due to extension generates a flatter and shallower basin (Figure 5d). If the extension is slow, vertical filling along the steepest hillslope is more pronounced (Figure 5f).

4.4 Effect of lithospheric thermal thickness

In our experiments, thermal lithospheric thickness, h_t, is defined according to the common definition, i.e., as the thickness of the conduction-dominated upper layer, different from the convection-dominated asthenosphere (Jaupart and Mareschal, 1999). We used surface heat flux values recorded by vitrinite reflectance to calculate the initial values of h_t. To test model sensitivity

to this parameter, additional experiments were implemented (Figure 3l), where h_t values were varied

from 60 km (reference experiment) to 85 km. The results show that MCCs form even for the largest

of the tested values of the lithospheric thickness. No significant difference is found in temporal

distribution and exhumation rates and styles except for some slight differences in Moho topography

(Figure 6). In all of these experiments, the continental lithosphere mantle extends homogeneously

and remains mechanically decoupled from the lower crust with no noticeable impact on Moho

geometry.

5. Discussion

5.1 Geometrical comparison with the observations

The Liaonan and Yiwulüshan MCCs are studied and described by several regional scaled

geological surveys (Charles et al., 2012; LBGMR, 1994; Lin et al., 2013a; Lin et al., 2013b; Liu et

al., 2005; Yin and Nie, 1996).Long-lasting multi-phase deformation are documented or suggested for

this region in the geological literature (Lin et al., 2013a). Here, we focused on the final stage of the

MCC deformation and did not consider the hypothetic relation between the Liaonan and Yiwulüshan

MCCs that may involve crustal rotation (Liu et al., 2005).

One of the experiments developed in this study (q_0=85 mW/m^2, V=0.33 cm/y, k_{ero}=500 m^2/y,

strain softening) (Figure 5b) is in good agreement with the characteristic features of the Liaonan

MCC structure, with a ~30-km-wide dome and moderate dipping angles of detachment (ca. 30° to

50°). A well-foliated mylonite/ultramylonite zone formed as a result of progressive grain size

reduction and preferential strain reorientation reasserts the importance of strain softening in the

formation of this MCC. For the Yiwulüshan MCC, the geometry of the syn-rift basin left-bounded by

the detachment has been interpreted based on seismic data (Wang et al., 1998). This interpretation depicts a 30-km-wide and 5-km-deep depression that is largely identical to that reproduced by the numerical model, although the latter has insufficient spatial resolution to reproduce the sedimentary sequences and the internal faults. The other side of the dome is covered by modern Eocene sediments, with identified early Cenozoic strata at the bottom (Qi and Yang, 2010). Thus, a small amount of the sedimentary deposits coeval to the MCC deformation is not excluded. For the Liaonan MCC, a bi-vergent crustal detachment is found at the south end. This detachment extends in a V-shape toward the north. However, its right limb may be below present sea level (Lin et al., 2008), and the affinity between the small basin and detachment is rather complex. Our synthetic simulations provide two possible conditions. One may be due to the extremely low rates of surface erosion. Another is that the small-scale basin represents a further denudation or late reformation at the surface that ultimately results in an exposure of a deeper level of the whole crust, where volcanic rocks are directly observable within the basin.

The Moho is situated at a depth of 27 km in our model, with a relatively small deflection (slope value <10°). Present-day topography data indicate a slightly greater depth (30 km), which can be related to additional flattening of the Moho boundary during post-rift thermal subsidence. Because all previous numerical models (e.g. Huet et al., 2011a; Tirel et al., 2008) have shown that thick crust favours MCC formation, we also carried out a series of experiments with a thicker initial crust to account for the eventual uncertainties of its estimation suggested by Ge et al. (2012) as well as for possible crustal thinning due to thermal erosion or other poorly constrained processes. These models did not show any significant differences from the experiments based on the assumption of an initially normal crustal thickness.

5.2 Geochronological comparison of model results with the observations

Previous geophysical and geological studies have provided a series of geochronological constraints based on closure temperatures of various minerals. A high heat flux (Fu et al., 2005) during the late Mesozoic proves the presence of hot crust (Moho temperature >800℃). Throughout this period, a "giant igneous event" is deemed a genetic link to lithospheric thinning. Several generations of Mesozoic plutons intrude in metamorphic rocks. Instead of addressing such timescales, we restrict the comparison to the metamorphic state of the dome. For the Liaonan MCC, the granitic intrusions were emplaced at 125-118 Ma, as shown by U-Pb zircon ages (Guo et al., 2004; Wu et al., 2005a). $^{40}Ar/^{39}Ar$ ages of muscovite, hornblende, biotite and k-feldspar obtained from mylonite and migmatites are within 120-107 Ma (Yang et al., 2007). The synthetic cooling rate calculated from the thermo-mechanical models (Figure 7a) is in good agreement with experimental results, with a closure temperature of hornblende at 500 °C (Harrison, 1981), muscovite at 350 °C (Hames and Bowring, 1994), biotite at 300°C (Harrison et al., 1985), and K-feldspar at 200 °C (Lovera et al., 1989). A fast cooling rate is derived from the thermal gradient of approximately 40-55 °C/my (Figure 7b), which is consistent with syn-tectonic granites reported in the eastern part of the NCC (Lin et al., 2011; Ratschbacher et al., 2000; Wang and Li, 2008; Yang et al., 2007; Yang et al., 2008). The Yiwulüshan MCC, with a two-phase 'fast' cooling rate (Lin et al., 2013a) is not compared here because strong constraints for geochronological work are lacking. The occurrence of rapid cooling in migmatite-cored complexes is attributed to high geothermal gradients generating convective fluid flow and exhumation-driving heat advection.

5.3 Predicted P-T-t paths of MCC

To trace the thermal and pressure trajectory of MCCs, we used passive markers (500 markers in

20

the lower crust) whose P-T conditions are systematically stored at each model step during the computations. The initial P-T conditions of the "exhumed" markers are found in the lower crust within the supra-solidus range, suggesting that the corresponding lower crustal units ever experienced partial melting due to their relatively high temperature at the onset of the extensional process. The markers are mostly located in the medium to low P/T metamorphic facies series characterized by granulite-amphibotite facies (Figure 8). These do not cross the P-T domain of eclogite or blueschist facies, which typically represent HP to UHP rocks undergoing an orogenic collisional event or that would be expected in subduction zones. The results of our experiments (with normal crust) are rather inconsistent with the evidence from "common" MCCs (Huet et al., 2011a; Schenker et al., 2012) for either isobaric heating or isothermal decompression close to the metamorphic peak. In contrast, our models predict a rapid cooling at a rate of >30°C/My on average. We propose that such a P-T path may be applicable to rocks originating from extremely high temperature but low pressure regions. Moreover, the predicted P-T-t paths are very sensitive to the extension rate. At a slow extension rate, the trajectory exhibits linear decompression and cooling so that a preferentially solid-state metamorphism occurs in the case of a slow strain rate. At a fast extension rate, a nearly isothermal decompression occurs, which is consistent with the most common MCC scenarios (Rey et al., 2009; Schenker et al., 2012).

5.4 Melting and phase changes

An elliptical migmatitic core lithologically consists of well-developed metatexites, with either leucosome or melanosome layering that exhibits significant partial melting. However, following Huet et al. (2011a, 2011b), we did not implement partial melting and phase changes in our experiments, even though the numerical code used in this study can account for these processes

(Angiboust et al., 2012; Burov and Gerya, 2014). Instead, in this study, we only estimated the initial melt fraction at a maximum of ~35% (Figure 8, inset) in the lower crust following the treatment from Schenker et al. (2012). This simplification is made due to the huge uncertainties of parameterization of the corresponding phenomena in crustal conditions. In particular, the metamorphic phase changes become largely metastable at temperatures below 500°C and largely depend on the amounts of free fluids. Similarly, the conditions for partial melting and melt migration are controlled by an abundance of poorly known factors, including fluid content, and dynamic strain and strain-dependent matrix permeability and porosity (Angiboust et al., 2012). In the absence of sufficient information in the NCC area, we have merely accounted for the effect of melting and phase changes by introducing strain-dependent brittle softening and varying the rheological properties of the ductile rocks.

6. Conclusions

Close similarities between the predictions of our numerical experiments, geological observations and cooling history evolution support the hypothesis of the possible development of a large-scale extension and MCCs in a non-over-thickened crust in the eastern NCC during the Late Mesozoic (Charles, 2010; Gumiaux et al., 2012; Lin et al., 2013a). In contrast with most previously published studies, we suggest that over-thickened orogenic crust is not a mandatory condition for MCC development. In particular, our study demonstrates the following:

1). There are two major modes of extension of hot non-over-thickened normal crusts: wide rifting and core complexes. The numerical thermo-mechanical models show that, under certain conditions, MCCs can develop on normal and non-over-thickened continental crust. These conditions basically indicate a high local geothermal gradient in the lithosphere, a rheologically stratified crust with a

weak ductile lower crust and a slow extension rate. MCC formation is consistently reproduced in the case of rheologically stratified crust with a weak lower crust and elevated Moho temperature (T>800℃).

2). The thickness of the mantle lithosphere only has a second-order effect on MCC development. In contrast, the crustal structure plays an important role in MCC development.

3). Strain softening provides an efficient mechanism for the development of crustal detachments rooted in the lower crust. The corresponding models demonstrate asymmetric deformation and topography evolution, while keeping the Moho surface nearly flat (compatible with the conventional definition of MCCs).

4). Surface erosion/sedimentation may induce separation of the syn-rift basin onto two basins: an "inactive" basin and an active supradetachment basin.

Table 1

Parameters applied in this study

	Rock	$\rho(kg\ m^{-3})$	$A(MPa^{-n}s^{-1})$	n	$H(kJ\ mol^{-1})$
Upper Crust	[1]Quartz-diorite	2800	1.26×10^{-3}	2.4	219
Lower Crust	[1]Quartz-diorite	2800	1.26×10^{-3}	2.4	219
	[2]Wet diorite	2800	3.2×10^{-2}	2.4	212
Mantle Lithosphere	[3]Olivine	3300	1×10^{4}	3	520
Compositional anomaly	[4]Granite	2600	3.2×10^{-2}	2.4	212
Sediment	Sediment	2300	1.26×10^{-3}	2.4	219

Gravity constant g (m s^{-1})	9.8
Friction angle φ (°)	30
Cohesion C_0 (MPa)	20
Young's modulus E (GPa)	80
Poisson ratio	0.25
Thermal conductivity k (W m^{-1} K^{-1})	2.5(k_c)/3.3(k_m)
Thermal expansion α (K^{-1})	3×10^{-5}
Adiabatic compressibility β (Pa^{-1})	8.065×10^{-12}
Radiogenic production decay depth h_r (km)	10
Internal heat production at surface H_s (W kg^{-1})	10^{-9}
Surface temperature T_0 (°C)	0
Bottom temperature T_b (°C)	1330
Surface heat flux q_0 (mW m^{-2})	75, 80, 85
Extension velocity V (cm y^{-1})	0.33, 0.66, 1
Coefficient of erosion k_{ero} (m^{2}a^{-1})	0, 100, 250, 500,750,1000

A, n, H are ductile flow laws parameters of lithospheric materials inherited from [1]Ranalli and Murphy (1987), [2]Ranally (1995) [3]Brace and Kohlstedt (1980), [4]Kirby and Kronenberg (1987).

Figure captions

Figure 1.(a) Structural map of the eastern part of China characterizing the NW-SE wide rift systems during the Late Mesozoic and Cenozoic. The MCC distribution is divided into two categories by UHP rocks constraints. See reference from Charles et al., (2012) and Lin et al., (2013a). HH: Hohhot; YM: Yunmengshan; FS: Fangshan; YW: Yiwulüshan; GD: Gudaoling; LN: Liaonan; LL: Linglon; LU: Lutian; HZ: Hongzhen; LS: Lushan; (b) Kinematic extension processes interpreted in the restoration of a crustal cross-section accounting for the possible contribution of thermal erosion (the pink line indicates the average lateral strain rate, the orange dot shows the initial crustal thickness of 35 km before the MCC exhumation and the long-term strain rate of the K_1s period (modified from Ge et al., 2012); (c) Cross-sections through the Yiwulüshan massif and Fuxin–Yixian basin (modified from Fig.3B from Lin et al., 2013a and see profile location therein); (d) Cross-sections within the Liaonan massif and Wafangdian half-graben (modified from Fig. 3c from Lin et al., 2008 and see profile location therein).

Figure 2. (a) Model setup (see description in the text, Table 1 and Appendix in supplementary material). Three initial thermal profiles corresponding to different tested values of lithospheric thickness. q_0 is the surface heat flux. Unilateral extension is applied at the right boundary (tested velocity range 0.33 to 1 cm/y). A prescribed initial intrusion (lower density) is located at a depth of 26-30 km. Bottom panel: rheological yield strength envelopes for different thermal gradients for (b) homogeneous crust and (c) stratified crust. Note the significance differences between the corresponding (e) effective viscosity profiles and the presence of a strong viscosity jump in the case of stratified crust (this jump results in an enhanced growth rate of extensional instabilities).

Figure 3. Snapshots of homogeneous (left column) and stratified (right column) models at times of

25

4.8, 9.6, and 22 Ma and q_0=85 mW/m^2. (b, d, f, h, j, l) Topography (a, c, e, g, i, k, colours refer to models with different thermal gradients shown in Figure 2). Note that the velocity is the same (0.33 cm/yr) in all experiments of this section.

Figure 4. Snapshots of the total shear stain distribution: formation (a-b) of a symmetric dome in the case of no strain softening and (c-d) formation of strongly asymmetric MCCs in the case of strain softening. Surface heat flux q_0=85mW/m^2 and boundary velocity V=0.33 cm/y. (e) Sequential topography variation of asymmetric MCCs. (f) Influence of the extension velocity (0.33, 0.66, 1cm/y) on the topography evolution.

Figure 5. (a-b) Snapshots of the results of the experiments with stratified crust, strain softening and surface erosion. Black solid lines represent shear zones whose geometries are obtained from total shear strain profiles. B1: Initial basin at the first stage of evolution. B2l: the left inactive basin and B2r: the right supradetachment basin, both at the second stage of evolution. The scale of the basin is characterized by the width and depth of continuously deposited sediments. Panels (c, e): Influence of the diffusion coefficient on the temporal variations in basin width. The one with 750 m^2/y which exhibits constant growth, may be caused by the abnormal insensibility to the surface load. In this scenario, the enlarged markers indicate the time of the superficial rupture of the basin within a narrow range of 2 Myrs (the grey shadow). Panels (d, f): Influence of the extension velocity on the temporal variation in the depth of the basin. In this scenario, the enlarged markers indicate the emergence of a third locus of uplift due to the ductile flow in the lower crust.

Figure 6. Effect of the lithospheric thickness on Moho undulation during the MCC deformation.

Figure 7. Model-predicted cooling rate compared with the experimental geochronological data from the Liaonan MCC. Flow paths of the passive markers are shown as pink lines in the phase diagrams.

Figure 8. Predicted P-T-t paths of the MCC. The passive markers are the same as those shown in Figure 7. The inset indicates the initial melt fraction at the crustal scale. Aluminium silicate stability diagram (dashed red line): Ky-kyanite, And-Andalusite, Sil-Sillimanite. PWS: politic wet solidus (Thompson, 1976), MS: muscovite + plagioclase + quartz = aluminumsilicate+ K-feldspar + liquid dehydration melting reaction (Thompson and Tracy, 1979), Pressure-temperature fields of metamorphic facies (dashed black line).

References

Angiboust, S., Wolf, S., Burov, E., Agard, P., Yamato, P., 2012. Effect of fluid circulation on subduction interface tectonic processes: Insights from thermo-mechanical numerical modelling. Earth and Planetary Science Letters 357, 238-248.

Brace, W. F., Kohlstedt, D.L., 1980. Limits on lithospheric stress imposed by laboratory experiments. Journal of Geophysical Research 85, 6248-6252.

Brun, J.P., 1999. Narrow rifts versus wide rifts: inferences for the mechanics of rifting from laboratory experiments. Philosophical Transactions of the Royal Society a-Mathematical Physical and Engineering Sciences 357, 695-710.

Brun, J.P., Sokoutis, D., 2007. Kinematics of the southern rhodope core complex (North Greece). International Journal of Earth Sciences 96, 1079-1099.

Buck, W.R., 1991. Modes of continental lithospheric extension. Journal of Geophysical Research-Solid Earth 96, 20161-20178.

Buck, W.R., 1993. Effect of lithospheric thickness on the formation of high-angle and low-angle normal faults. Geology 21, 933-936.

Burov, E., 2007. The role of gravitational instabilities, density structure and extension rate in the evolution of continental margins, in: Karner, G.D., Manatschal, G., Pinheiro, L.M. (Eds.), Imaging, mapping and modelling continental lithosphere extension and breakup. Geological Society Special Publications, London, pp. 139-156.

Burov, E., 2011. Rheology and strength of the lithosphere. Marine and Petroleum Geology 28, 1402-1443.

Burov, E., Cloetingh, S., 2010. Plume-like upper mantle instabilities drive subduction initiation. Geophysical Research Letters 37.

Burov, E., Diament, M., 1995. The effective elastic thickness (Te) of continental lithosphere - What does it really mean. Journal of Geophysical Research-Solid Earth 100, 3905-3927.

Burov, E., Francois, T., Agard, P., Le Pourhiet, L., Meyer, B., Tirel, C., Lebedev, S., Yamato, P., Brun, J.P., 2014. Rheological and geodynamic controls on the mechanisms of subduction and HP/UHP exhumation of crustal rocks during continental collision: Insights from numerical models. Tectonophysics 631, 212-250.

Burov, E., Gerya, T., 2014. Asymmetric three-dimensional topography over mantle plumes. Nature 513, 85-89.

Burov E., Houdry, F., Diament, M., Déverchère, J., 1994. A broken plate beneath the North Baikal rift zone revealed by gravity modelling. Geophysical Research Letters 21, 129-132.

Burov, E., Poliakov, A., 2001. Erosion and rheology controls on synrift and postrift evolution: Verifying old and new ideas using a fully coupled numerical model. Journal of Geophysical ResearchSolid Earth 106, 16461-16481.

Burov, E., Poliakov, A., 2003. Erosional forcing of basin dynamics: new aspects of syn- and post-rift evolution. New Insights into Structural Interpretation and Modelling 212, 209-223.

Burov, E., Yamato, P., 2008. Continental plate collision, P-T-t-z conditions and unstable vs. stable plate dynamics: Insights from thermo-mechanical modelling. Lithos 103, 178-204.

Byerlee, J., 1978. Friction of rocks. Pure and Applied Geophysics 116, 615-626.

Charles, N., 2010. Mécanismes de l'extension continentale au Mésozoïque en Asie de l'Est, PhD thesis. Université d'Orléans, France, pp. 476.

Charles, N., Augier, R., Gumiaux, C., Monie, P., Chen, Y., Faure, M., Zhu, R.X., 2013. Timing, duration and

role of magmatism in wide rift systems: Insights from the Jiaodong Peninsula (China, East Asia). Gondwana Research 24, 412-428.

Charles, N., Chen, Y., Augier, R., Gumiaux, C., Lin, W., Faure, M., Monie, P., Choulet, F., Wu, F.Y., Zhu, R.X., Wang, Q.C., 2011a. Palaeomagnetic constraints from granodioritic plutons (Jiaodong Peninsula): New insights on Late Mesozoic continental extension in Eastern Asia. Physics of the Earth and Planetary Interiors 187, 276-291.

Charles, N., Gumiaux, C., Augier, R., Chen, Y., Faure, M., Lin, W., Zhu, R.X., 2012. Metamorphic Core Complex dynamics and structural development: Field evidences from the Liaodong Peninsula (China, East Asia). Tectonophysics 560, 22-50.

Charles, N., Gumiaux, C., Augier, R., Chen, Y., Zhu, R.X., Lin, W., 2011b. Metamorphic Core Complexes vs. synkinematic plutons in continental extension setting: Insights from key structures (Shandong Province, eastern China). Journal of Asian Earth Sciences 40, 261-278.

Chen, J., Cai, X., C., L., Wang, H., Lei, M., 1999. Tectonic characteristics and episodic evolution of the northern fault depression in Songliao Basin (in Chinese with English abstract). Acta Petrolei Sinica 20, 14-18.

Chen, L., Tao, W., Zhao, L., Zheng, T.Y., 2008. Distinct lateral variation of lithospheric thickness in the northeastern North China Craton. Earth and Planetary Science Letters 267, 56-68.

Chen, L., Zheng, T.Y., Xu, W.W., 2006. Receiver function migration image of the deep structure in the Bohai Bay Basin, eastern China. Geophysical Research Letters 33.

Coney, P.J., 1974. Structural-analysis of Snake Range Decollement East-Central Nevada. Geological Society of America Bulletin 85, 973-977.

Coney, P.J., Harms, T.A., 1984. Cordilleran metamorphic core complexes: Cenozoic extensional relics of Mesozoic compression. Geology 12, 550-554.

Cong, B., 1996. Ultrahigh-pressure Metamorphic rocks in the Dabieshan– Sulu region of China. Eds. Science Press, Beijing.

Culling, W., 1960. Analytical theory of erosion. The Journal of Geology, 336-344.

Cundall, P.A., 1989. Numerical experiments on localization in frictional materials. Ingenieur Archiv 59, 148-159.

Davis, G.H., Coney, P.J., 1979. Geologic development of the Cordilleran metamorphic core complexes. Geology 7, 120-124.

Davis, G.A., Zheng, Y.D., 1988. A possible cordilleran-type metamorphic core complex beneath the Great Wall near Hefangkou, Huairou County, northern China. Geological Society of America Abstracts with Programs 20, Abstract 324.

Darby, B.J., Davis, G.A., Zheng, Y.D., Zhang, J., Wang, X., 2001. Evolving geometry of the Hohhot metamorphic core complex, Inner Mongolia, China. Geological Society of America Abstracts with Programs 33,32-32.

Donskaya, V., Windley, B.F., Mazukabzov, M., Kroner, A., Sklyarov, E.V., Gladkochub, D.P., Ponomarchuk, V.A., Badarch, G., Reichow, M.K., Hegner, E., 2008. Age and evolution of late Mesozoic metamorphic core complexes in southern Siberia and northern Mongolia. Journal of the Geological Society 165, 405–421.

Faure, M., Lin, W., Scharer, U., Shu, L.S., Sun, Y., Arnaud, N., 2003. Continental subduction and exhumation of UHP rocks. Structural and geochronological insights from the Dabieshan (East China). Lithos 70, 213-241.

Foster, D.A., Raza, A., 2002. Low-temperature thermochronological record of exhumation of the Bitterroot

metamorphic core complex, northern Cordilleran Orogen. Tectonophysics 349, 23-36.

Fu, M.X., Hu, S.B., Wang, J.Y., 2005. Thermal regime transition in eastern North China and its tectonic implication. Science in China Series D-Earth Sciences 48, 840-848.

Gautier, P., Ballevre, M., Brun, J.P., Jolivet, L., 1990. Ductile extension and sedimentary basins of Mio-Pliocene age in the Cyclades (Islands of Naxos and Paros). Comptes Rendus De L'Academie Des Sciences Serie Ii 310, 147-153.

Gautier, P., Brun, J.P., Jolivet, L., 1993. Structure and Kinematics of Upper Cenozoic extensional detachment on Naxos and Paros (Cyclades Islands, Greece). Tectonics 12, 1180-1194.

Ge, R.F., Zhang, Q.L., Wang, L.S., Chen, J., Xie, G.A., Wang, X.Y., 2012. Late Mesozoic rift evolution and crustal extension in the central Songliao Basin, northeastern China: constraints from cross-section restoration and implications for lithospheric thinning. International Geology Review 54, 183-207.

Gebelin, A., Mulch, A., Teyssier, C., Heizler, M., Vennemann, T., Seaton, N.C.A., 2011. Oligo-Miocene extensional tectonics and fluid flow across the Northern Snake Range detachment system, Nevada. Tectonics 30.

Gessner, K., Wijns, C., Moresi, L., 2007. Significance of strain localization in the lower crust for structural evolution and thermal history of metamorphic core complexes. Tectonics 26.

Graham, S. A., Hendrix, M.S., Johnson, C.L., Badamgarav, D., Badarch, G., Amory, J., Porte, M., Barsbold, R.,Webb, L.E., Hacker, B.R., 2001. Sedimentary record and tectonic implications of Mesozoic rifting in southern Mongolia.Geological Society of America Bulletin113, 1560-1579.

Griffin, W.L., Andi, Z., O'Reilly, S.Y., Ryan, C.G., 1998. Phanerozoic evolution of the lithosphere beneath the Sino-Korean Craton. Mantle Dynamics and Plate Interactions in East Asia 27, 107-126.

Gumiaux, C., Charles, N., Augier, R., Chen, Y., Faure, M., 2012. Can metamorphic core complexes develop within a previously non-thickened crust? Insights from the North China Late Mesozoic continental extension, EGU General Assembly Conference Abstracts, p. 12395.

Guo, C.L., Wu, F.Y., Yang, J.H., Lin, J.Q., Sun, D.Y., 2004. The extensional setting of the Early Cretaceous magmatism in eastern China: example from the Yinmawanshan pluton in southern Liaodong Peninsula. Acta Petrologica Sinica 20, 1193-1204.

Hames, W.E., Bowring, S.A., 1994. An Empirical-Evaluation of the Argon Diffusion Geometry in Muscovite. Earth and Planetary Science Letters 124, 161-167.

Hao, T.Y., Yang, C.C., Liu, H., Song, H.B., Jiang, W.W., 2007. Integrated geological and geophysical study for pre-cenozoic hydrocarbon resources in the circum-bohai area (in Chinese with English abstract). Progress in Geophysics 22, 1269-1279.

Harrison, T.M., 1981. Diffusion of Ar-40 in Hornblende. Contributions to Mineralogy and Petrology 78, 324-331.

Harrison, T.M., Duncan, I., Mcdougall, I., 1985. Diffusion of Ar-40 in biotite - temperature, pressure and compositional effects. Geochimica Et Cosmochimica Acta 49, 2461-2468.

Hu, S.B., He, L.J., Wang, J.Y., 2000. Heat flow in the continental area of China: a new data set. Earth and Planetary Science Letters 179, 407-419.

Huet, B., Le Pourhiet, L., Labrousse, L., Burov, E., Jolivet, L., 2011a. Post-orogenic extension and metamorphic core complexes in a heterogeneous crust: the role of crustal layering inherited from collision. Application to the Cyclades (Aegean domain). Geophysical Journal International 184, 611-625.

Huet, B., Le Pourhiet, L., Labrousse, L., Burov, E.B., Jolivet, L., 2011b. Formation of metamorphic core complex in inherited wedges: A thermomechanical modelling study. Earth and Planetary Science

Letters 309, 249-257.

Huismans, R.S., Beaumont, C., 2003. Symmetric and asymmetric lithospheric extension: Relative effects of frictional-plastic and viscous strain softening. Journal of Geophysical Research-Solid Earth 108, 1978-2012.

Huismans, R.S., Buiter, S.J.H., Beaumont, C., 2005. Effect of plastic-viscous layering and strain softening on mode selection during lithospheric extension. Journal of Geophysical Research-Solid Earth 110.

Jaupart, C., Mareschal, J.C., 1999. The thermal structure and thickness of continental roots. Lithos 48, 93-114.

Jolivet, L., Faccenna, C., 2000. Mediterranean extension and the Africa-Eurasia collision. Tectonics 19, 1095-1106.

Jolivet, L., Faccenna, C., Huet, B., Labrousse, L., Le Pourhiet, L., Lacombe, O., Lecomte, E., Burov, E., Denele, Y., Brun, J.P., Philippon, M., Paul, A., Salaun, G., Karabulut, H., Piromallo, C., Monie, P., Gueydan, F., Okay, A.I., Oberhansli, R., Pourteau, A., Augier, R., Gadenne, L., Driussi, O., 2013. Aegean tectonics: Strain localisation, slab tearing and trench retreat. Tectonophysics 597, 1-33.

Kirby, S. H., Kronenberg, A.K., 1987. Rheology of the lithosphere: Selected topics. Review of Geophysics 25, 1219-1244

Lavier, L.L., Buck, W.R., 2002. Half graben versus large-offset low-angle normal fault: Importance of keeping cool during normal faulting. Journal of Geophysical Research-Solid Earth 107.

Lavier, L.L., Buck, W.R., Poliakov, A.N.B., 1999. Self-consistent rolling-hinge model for the evolution of large-offset low-angle normal faults. Geology 27, 1127-1130.

LBGMR (Liaoning Bureau of Geology and Mineral Resources), 1989. Regional Geology of Liaoning Province (in Chinese with English summary). Geological Publishing House, Beijing, 856 pp.

Le Pourhiet, L., Burov, E., Moretti, I., 2004. Rifting through a stack of inhomogeneous thrusts (the dipping pie concept). Tectonics 23.

Le Pourhiet, L., Huet, B., May, D.A., Labrousse, L., Jolivet, L., 2012. Kinematic interpretation of the 3D shapes of metamorphic core complexes. Geochemistry Geophysics Geosystems 13.

Li, S.L., Mooney, W.D., Fan, J.C., 2006. Crustal structure of mainland China from deep seismic sounding data. Tectonophysics 420, 239-252.

Li, W.B., 2001. Palynoflora from the Quantou Formation of Songliao Basin, NE China and its bearing on the Upper-Lower Cretaceous boundary (in Chinese with English abstract). Acta Palaeontologica Sinica 40, 166-176.

Li, X.H., 2000. Cretaceous magmatism and lithospheric extension in Southeast China. Journal of Asian Earth Sciences 18, 293-305.

Lin, W., Charles, N., Chen, Y., Chen, K., Faure, M., Wu, L., Wang, F., Li, Q.L., Wang, J., Wang, Q.C., 2013b. Late Mesozoic compressional to extensional tectonics in the Yiwulushan massif, NE China and their bearing on the Yinshan-Yanshan orogenic belt Part II: Anisotropy of magnetic susceptibility and gravity modeling. Gondwana Research 23, 78-94.

Lin, W., Faure, M., Chen, Y., Ji, W.B., Wang, F., Wu, L., Charles, N., Wang, J., Wang, Q.C., 2013a. Late Mesozoic compressional to extensional tectonics in the Yiwulushan massif, NE China and its bearing on the evolution of the Yinshan-Yanshan orogenic belt Part I: Structural analyses and geochronological constraints. Gondwana Research 23, 54-77.

Lin, W., Faure, M., Monie, P., Scharer, U., Panis, D., 2008. Mesozoic extensional tectonics in eastern Asia: The south Liaodong Peninsula metamorphic core complex (NE China). Journal of Geology 116, 134-154.

Lin, W., Faure, M., Monie, P., Scharer, U., Zhang, L.S., Sun, Y., 2000. Tectonics of SE China: New insights

from the Lushan massif (Jiangxi Province). Tectonics 19, 852-871.

Lin, W., Faure, M., Monie, P., Wang, Q.C., 2007. Polyphase Mesozoic tectonics in the eastern part of the North China Block: insights from the eastern Liaoning Peninsula massif (NE China) (in Mesizoic sub-continental lithospheric thinning under eastern Asia) Geological Society Special Publications 280, 153-170.

Lin, W., Wang, Q., Wang, J., Wang, F., Chu, Y., Chen, K., 2011. Late Mesozoic extensional tectonics of the Liaodong Peninsula massif: Response of crust to continental lithosphere destruction of the North China Craton. Science China Earth Sciences 54, 843-857.

Lister, G.S., 1984. Metamorphic Core Complexes of Cordilleran Type in the Cyclades, Aegean Sea, Greece. Geology 12, 221-225.

Lister, G.S., Davis, G.A., 1989. The Origin of Metamorphic Core Complexes and Detachment Faults Formed during Tertiary Continental Extension in the Northern Colorado River Region, USA. Journal of Structural Geology 11, 65-94.

Liu, J.L., Davis, G.A., Lin, Z.Y., Wu, F.Y., 2005. The Liaonan metamorphic core complex, Southeastern Liaoning Province, North China: A likely contributor to Cretaceous rotation of Eastern Liaoning, Korea and contiguous areas. Tectonophysics 407, 65-80.

Lovera, O.M., Richter, F.M., Harrison, T.M., 1989. The Ar-40 Ar-39 Thermochronometry for Slowly Cooled Samples Having a Distribution of Diffusion Domain Sizes. Journal of Geophysical Research-Solid Earth and Planets 94, 17917-17935.

Mattauer, M., Matte, P., Malavielle, J., Tapponnier, P. Maluski, H., Xu, Z.Q., Lu, Y.L., Tang, Y.Q., 1985. Tectonics of Qinling belt: Build-up and evolution of western Asia. Nature 317, 496-500.

Meng, Q.R., 2003. What drove late Mesozoic extension of the northern China–Mongolia tract?. Tectonophysics 369, 155-174.

Menzies, M.A., Fan, W., Zhang, M., 1993. Palaeozoic and Cenozoic lithoprobes and the loss of> 120 km of Archaean lithosphere, Sino-Korean craton, China. Geological Society, London, Special Publications 76, 71-81.

Mulch, A., Teyssier, C., Cosca, M.A., Chamberlain, C.P., 2007. Stable isotope paleoaltimetry of Eocene core complexes in the North American Cordillera. Tectonics 26.

Parsons, B., Sclater, J.G., 1977. An analysis of the variation of ocean floor bathymetry and heat flow with age. Journal of Geophysical Research 82, 803-827.

Petit, C., Burov, E.,Déverchère, J., 1997. On the structure and the mechanical behaviour of the extending lithosphere in the Baikal Rift from gravity modeling. Earth and Planet Science Letters 149, 29-42.

Poliakov, A.N.B., Podladchikov, Y., Talbot, C., 1993. Initiation of Salt Diapirs with Frictional Overburdens - Numerical Experiments. Tectonophysics 228, 199-210.

Proffett, J.M., 1977. Cenozoic geology of Yerington District, Nevada, and implications for nature and origin of basin and range faulting. Geological Society of America Bulletin 88, 247-266.

Qi, J.F., Yang, Q., 2010. Cenozoic structural deformation and dynamic processes of the Bohai Bay basin province, China. Marine and Petroleum Geology 27, 757-771.

Ranalli, G.,1995. Rheology of the Earth. 2nd ed. Chapman and Hall, London, 413 pp.

Ranalli, G., Murphy, D.C., 1987. Rheological stratification of thelithosphere. Tectonophysics 132, 281-295.

Ratschbacher, L., Hacker, B.R., Webb, L.E., McWilliams, M., Ireland, T., Dong, S., Calvert, A., Chateigner, D., Wenk, H.R., 2000. Exhumation of the ultrahigh-pressure continental crust in east central China: Cretaceous and Cenozoic unroofing and the Tan-Lu fault. Journal of Geophysical Research-Solid Earth 105, 13303-13338.

Ren, J.Y., Tamaki, K., Li, S.T., Junxia, Z., 2002. Late Mesozoic and Cenozoic rifting and its dynamic setting in Eastern China and adjacent areas. Tectonophysics 344, 175-205.

Rey, P.F., Teyssier, C., Whitney, D.L., 2009. Extension rates, crustal melting, and core complex dynamics. Geology 37, 391-394.

Richard, S.M., Smith, C.H., Kimbrough, D.L., Fitzgerald, P.G., Luyendyk, B.P., Mcwilliams, M.O., 1994. Cooling history of the Northern Ford Ranges, Marie Byrd Land, West Antarctica. Tectonics 13, 837-857.

Schenker, F.L., Gerya, T., Burg, J.P., 2012. Bimodal behavior of extended continental lithosphere: Modeling insight and application to thermal history of migmatitic core complexes. Tectonophysics 579, 88-103.

Sklyarov, E.V., Mazukabzov, A.M., Melnikov, A.I., 1997. Metamorphic Core Complexes of the Cordilleran Type (in Russian), edited by F. A. Letnikov. SPC UIGGM Siberian Branch of the RAS, Novosibirsk, Russia, pp. 168–182.

Steltenpohl, M.G., Hames, W.E., Andresen, A., 2004. The Silurian to Permian history of a metamorphic core complex in Lofoten, northern Scandinavian Caledonides. Tectonics 23.

Thompson, A., Tracy, R., 1979. Model systems for anatexis of pelitic rocks. Contributions to Mineralogy and Petrology 70, 429-438.

Thompson, P.H., 1976. Isograd patterns and pressure-temperature distributions during regional metamorphism. Contributions to Mineralogy and Petrology 57, 277-295.

Tirel, C., Brun, J.-P., Burov, E., 2004. Thermomechanical modeling of extensional gneiss domes, in: Whitney, D.L., Teyssier, C., Siddoway, C.S. (Eds.), Gneiss domes and orogeny. Geological Society of America Special Paper, pp. 67-78.

Tirel, C., Brun, J.P., Burov, E., 2008. Dynamics and structural development of metamorphic core complexes, Journal of Geophysical Research-Solid Earth.

Tirel, C., Brun, J.P., Burov, E., Wortel, M.J.R., Lebedev, S., 2013. A plate tectonics oddity: Caterpillar-walk exhumation of subducted continental crust. Geology 41, 555-558.

Toussaint, G., Burov, E., Jolivet, L., 2004. Continental plate collision: Unstable vs. stable slab dynamics. Geology 32, 33-36.

Turcotte, D., Schubert, G., 1982. Geodynamics, 2nd ed. John Wiley, New York.

Verdel, C., Wernicke, B.P., Ramezani, J., Hassanzadeh, J., Renne, P.R., Spell, T.L., 2007. Geology and thermochronology of Tertiary Cordilleran-style metamorphic core complexes in the Saghand region of central Iran. Geological Society of America Bulletin 119, 961-977.

Wang, F., Zhou, X.H., Zhang, L.C., Ying, J.F., Zhang, Y.T., Wu, F.Y., Zhu, R.X., 2006. Late mesozoic volcanism in the Great Xing'an range (NE China): Timing and implications for the dynamic setting of NE Asia. Earth and Planetary Science Letters 251, 179-198.

Wang, L.G., Qiu, Y.M., McNaughton, N.J., Groves, D.I., Luo, Z.K., Huang, J.Z., Miao, L.C., Liu, Y.K., 1998. Constraints on crustal evolution and gold metallogeny in the Northwestern Jiaodong Peninsula, China, from SHRIMP U-Pb zircon studies of granitoids. Ore Geology Reviews 13, 275-291.

Wang, P.J., Liu, W.Z., Wang, S.X., Song, W.H., 2002. Ar-40/Ar-39 and K/Ar dating on the volcanic rocks in the Songliao basin, NE China: constraints on stratigraphy and basin dynamics. International Journal of Earth Sciences 91, 331-340.

Wang, T., Zheng, Y.D., Zhang, J.J. Zeng, L.S. Donskaya, T., Guo, L., Li, J.B., 2011. Pattern and kinematic polarity of late Mesozoic extension in continental NE Asia: perspectives from metamorphic core complexes.Tectonics 30.

Wang, W., Lu, S., Guo, Y., Sun, Y., 1998. Tectonic geometry and type of traps in Fuxin Basin. Journal of the

University of Petroleum 22, 26–30.

Wang, X.D., Neubauer, F., Genser, J., Yang, W., 1998. The Dabie UHP unit, Central China: A Cretaceous extensional alochthon superposed on a Triasic orogen. Tera Nova 10, 260-267.

Wang, X. S., Zheng, Y.D., Jia, W., 2004. Extensional stages of Louzidian metamorphic core complex and development of the Supra- detachment basin south of Chifeng, Inner Mongolia, China. Dizhi Xuebao 78, 237-245.

Wang, Y., Li, H.M., 2008. Initial formation and mesozoic tectonic exhumation of an intracontinental tectonic belt of the northern part of the Taihang Mountain Belt, eastern Asia. Journal of Geology 116, 155-172.

Watremez, L., Burov, E., d'Acremont, E., Leroy, S., Huet, B., LePourhiet, L., Bellahsen, N., 2013. Buoyancy and localizing properties of continental mantle lithosphere: Insights from thermomechanical models of the eastern Gulf of Aden. Geochemistry Geophysics Geosystems 14, 2800-2817.

Webb, L. E., Graham, S.A., Johnson, C.L., Badarch, G., Hendrix, M.S., 1999. Occurrence, age, and implication of the Yaga-Onch Hayrhan metamorphic core complex, southern Mongolia. Geology 27, 143-146.

Wei, Z.G., Chen, L., 2012. Regional differences in crustal structure beneath northeastern China and northern North China Craton: constraints from crustal thickness and V_p/V_s ratio. Chinese Jounal of Geophysics (in Chinese with English abstract) 55, 3601-3614.

Wernicke, B., 1981. Low-angle normal faults in the Basin and Range Province: Nappe tectonics in an extending orogen. Nature 291, 645-648.

Wu, F.Y., Han, R.H., Yang, J.H., Wilde, S.A., Zhai, M.G., Park, S.C., 2007. Initial constraints on the timing of granitic magmatism in North Korea using U-Pb zircon geochronology. Chemical Geology 238, 232-248.

Wu, F.Y., Jahn, B.M., Wilde, S., Sun, D.Y., 2000.Phanerozoic crustal growth: U-Pb and Sr-Nd isotopic evidence from the granites in northeastern China. Tectonophysics 328, 89-113

Wu, F.Y., Lin, J.Q., Wilde, S.A., Zhang, X.O., Yang, J.H., 2005a. Nature and significance of the Early Cretaceous giant igneous event in eastern China. Earth and Planetary Science Letters 233, 103-119.

Wu, F.Y., Yang, J.H., Wilde, S.A., Zhang, X.O., 2005b. Geochronology, petrogenesis and tectonic implications of Jurassic granites in the Liaodong Peninsula, NE China. Chemical Geology 221, 127-156.

Xiao, W.J., Windley, B.F., Hao, J., Zhai, M.G., 2003. Accretion lead- ing to collision and the Permian Solonker suture, Inner Mongolia, China: Termination of the Central Asian Orogenic Belt. Tectonics, 22.

Yamato, P., Agard, P., Burov, E., Le Pourhiet, L., Jolivet, L., Tiberi, C., 2007. Burial and exhumation in a subduction wedge: Mutual constraints from thermomechanical modeling and natural P-T-t data (Schistes Lustres, western Alps), Journal of Geophysical Research-Solid Earth.

Yamato, P., Mouthereau, F., Burov, E., 2009. Taiwan mountain building: insights from 2-D thermomechanical modelling of a rheologically stratified lithosphere. Geophysical Journal International 176, 307-326.

Yang, J.H., Wu, F.Y., Chung, S.L., Lo, C.H., 2008. The extensional geodynamic setting of Early Cretaceous granitic intrusions in the Eastern North China Craton: Evidence front laser ablation Ar-40/Ar-39 dating of K-bearing minerals. Acta Petrologica Sinica 24, 1175-1184.

Yang, J.H., Wu, F.Y., Chung, S.L., Lo, C.H., Wilde, S.A., Davis, G.A., 2007. Rapid exhumation and cooling of the Liaonan metamorphic core complex: Inferences from Ar-40/Ar-39 thermochronology and implications for Late Mesozoic extension in the eastern North China Craton. Geological Society of America Bulletin 119, 1405-1414.

Yin, A., Nie, S.Y., 1996. A Phanerozoic palinspastic reconstruction of China and its neighboring regions, in:

Yin, A., Harrison, T.A. (Eds.), The Tectonic Evolution of Asia. World and Regional Geology, New York, pp. 442-485.

Zhai, M.G., Zhu, R.X., Liu, J.M., Meng, Q.R., Hou, Q.L., Hu, S.B., Liu, W., Li, Z., Zhang, H.F., Zhang, H.F., 2004. Time range of Mesozoic tectonic regime inversion in eastern North China Block. Science in China Series D-Earth Sciences 47, 151-159.

Zhang, J.J, Zheng, Y.D., Shi, Q.,Yu, X., Zhang, Q., 1997. The Xiaoqinling detachment fault and metamorphic core complex of China: Structures, kinematics, strain and evolution. Procedings of the 30th International Geological Congres 14, 158-172.

Zhao, G.C., Wilde, S.A., Cawood, P.A., Sun, M., 2001. Archean blocks and their boundaries in the North China Craton: lithological, geochemical, structural and P-T path constraints and tectonic evolution. Precambrian Research 107, 45-73.

Zhao, L., Allen, R.M., Zheng, T.Y., Hung, S.H., 2009. Reactivation of an Archean craton: Constraints from P- and S-wave tomography in North China. Geophysical Research Letters 36.

Zhao, L., Allen, R.M., Zheng, T.Y., Zhu, R.X., 2012. High-resolution body wave tomography models of the upper mantle beneath eastern China and the adjacent areas. Geochemistry Geophysics Geosystems 13.

Zhao, L., Zheng, T.Y., Lu, G., 2013. Distinct upper mantle deformation of cratons in response to subduction: Constraints from SKS wave splitting measurements in eastern China. Gondwana Research 23, 39-53.

Zheng, T.Y., Zhao, L., Xu, W.W., Zhu, R.X., 2008. Insight into modification of North China Craton from seismological study in the Shandong Province. Geophysical Research Letters 35.

Zheng, T.Y., Zhao, L., Zhu, R.X., 2009. New evidence from seismic imaging for subduction during assembly of the North China craton. Geology 37, 395-398.

Zhu, G., Xie, C.L., Chen, W., Xiang, B.W., Hu, Z.Q., 2010. Evolution of the Hongzhen metamorphic core complex: Evidence for Early Cretaceous extension in the easternYangtze craton, eastern China. Geological Society of America Buletin 12. 506-516.

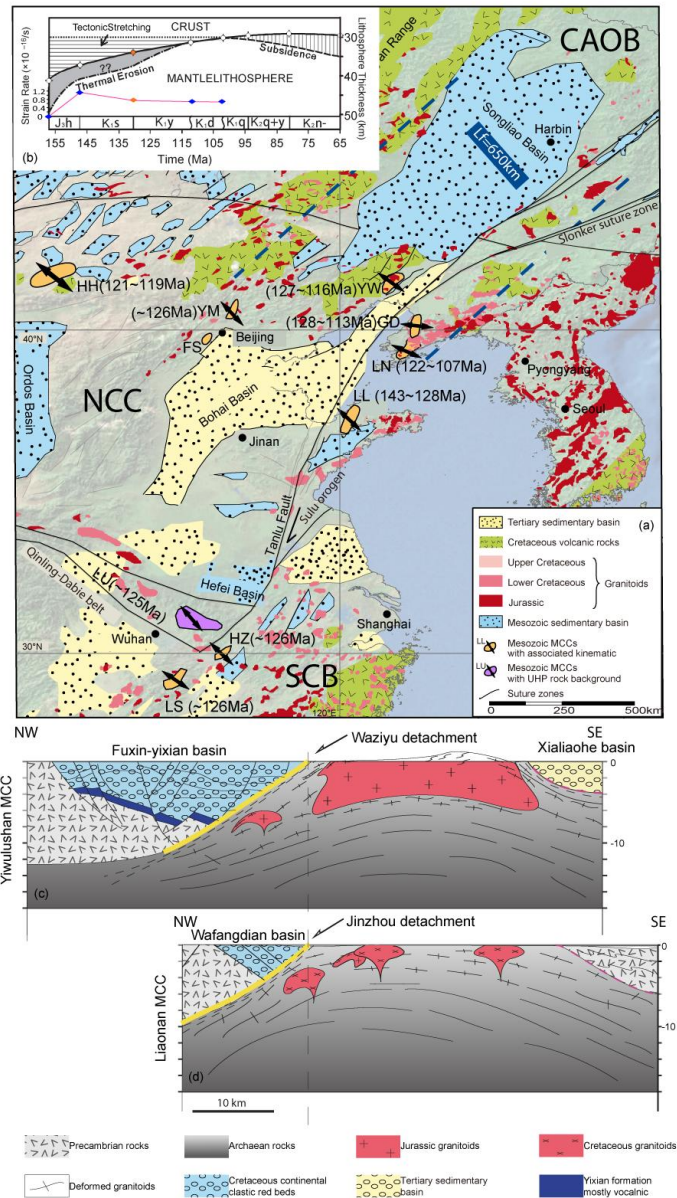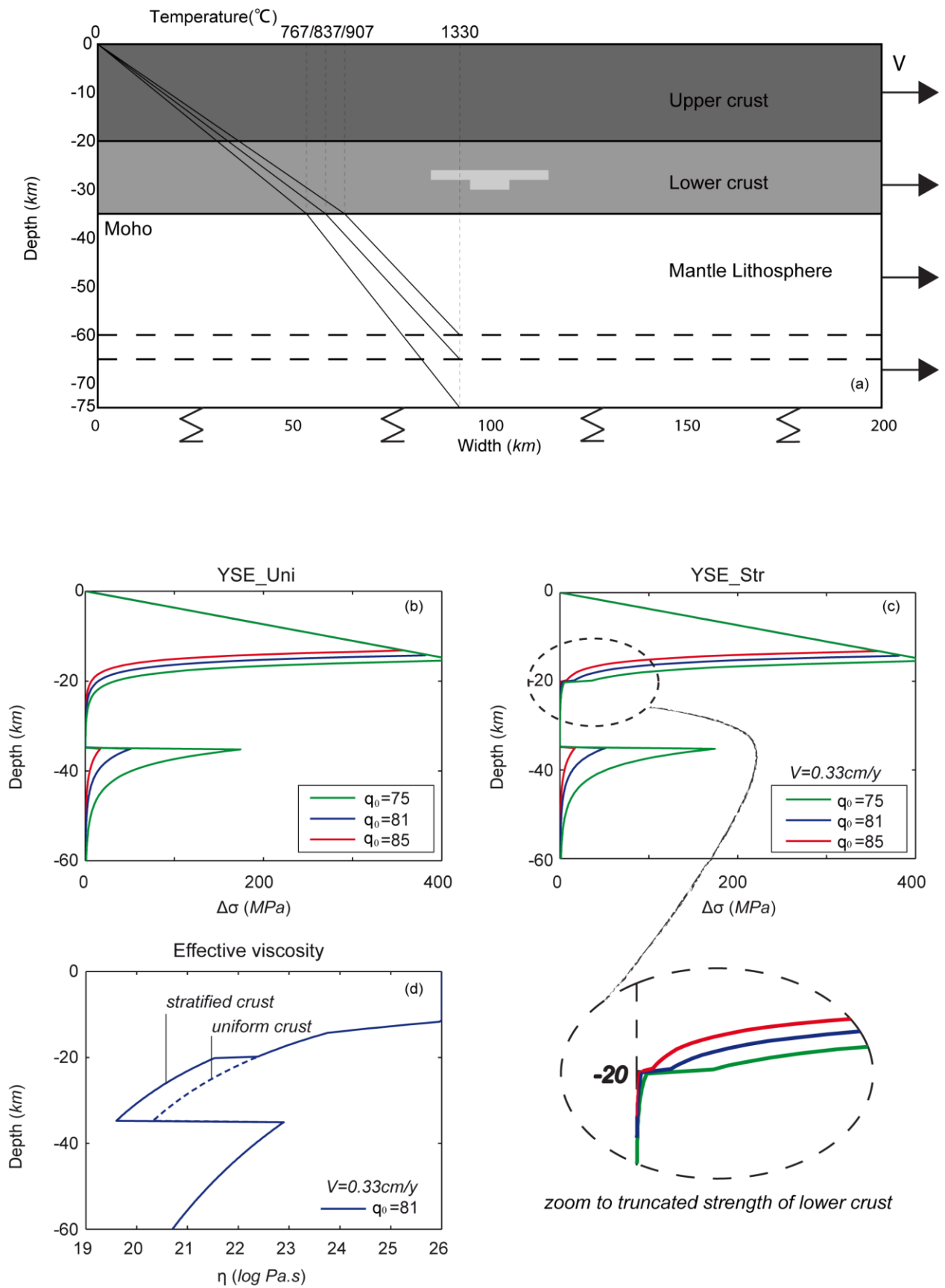Zhu, R.X., Xu, Y.G., Zhu, G., Zhang, H.F., Xia, Q.K., Zheng, T.Y., 2012. Destruction of the North China Craton. Science China-Earth Sciences 55, 1565-1587.
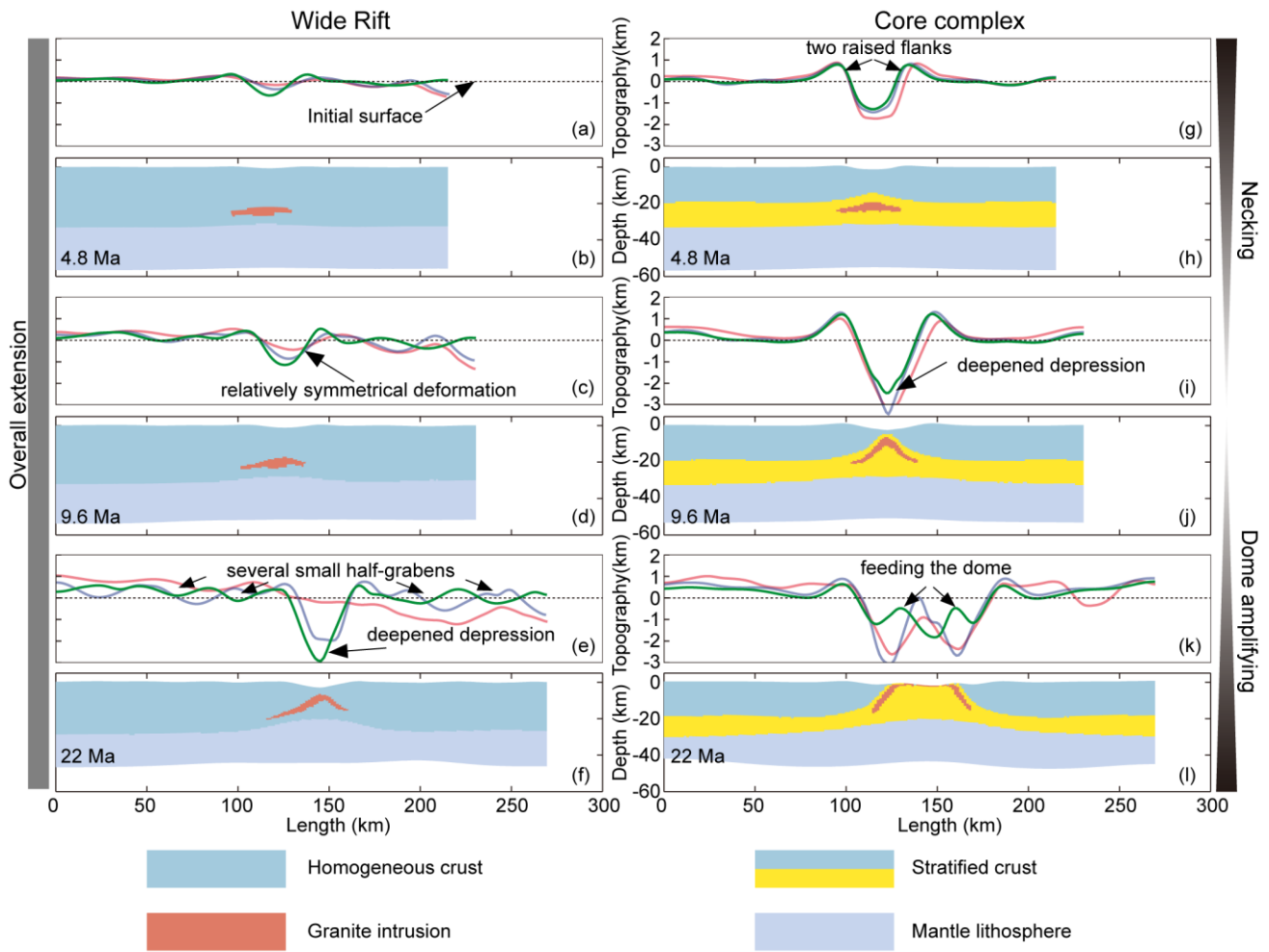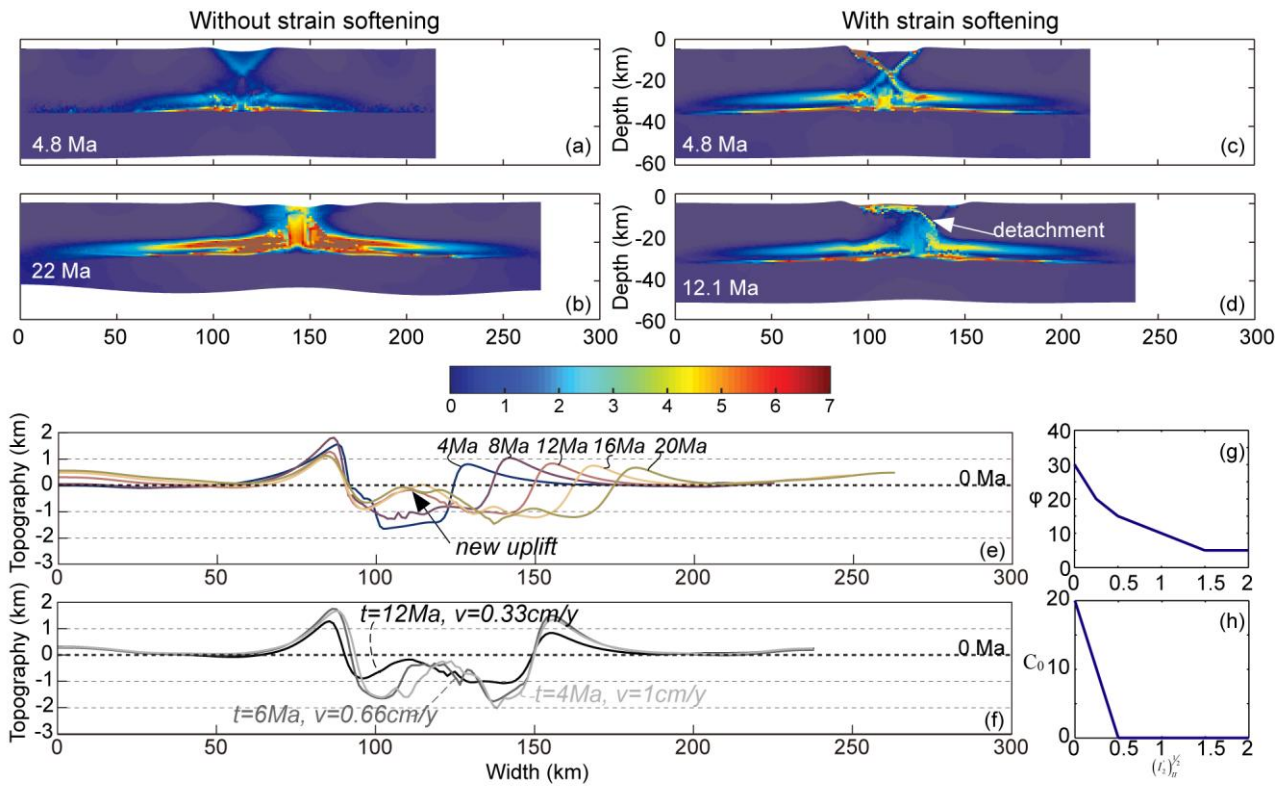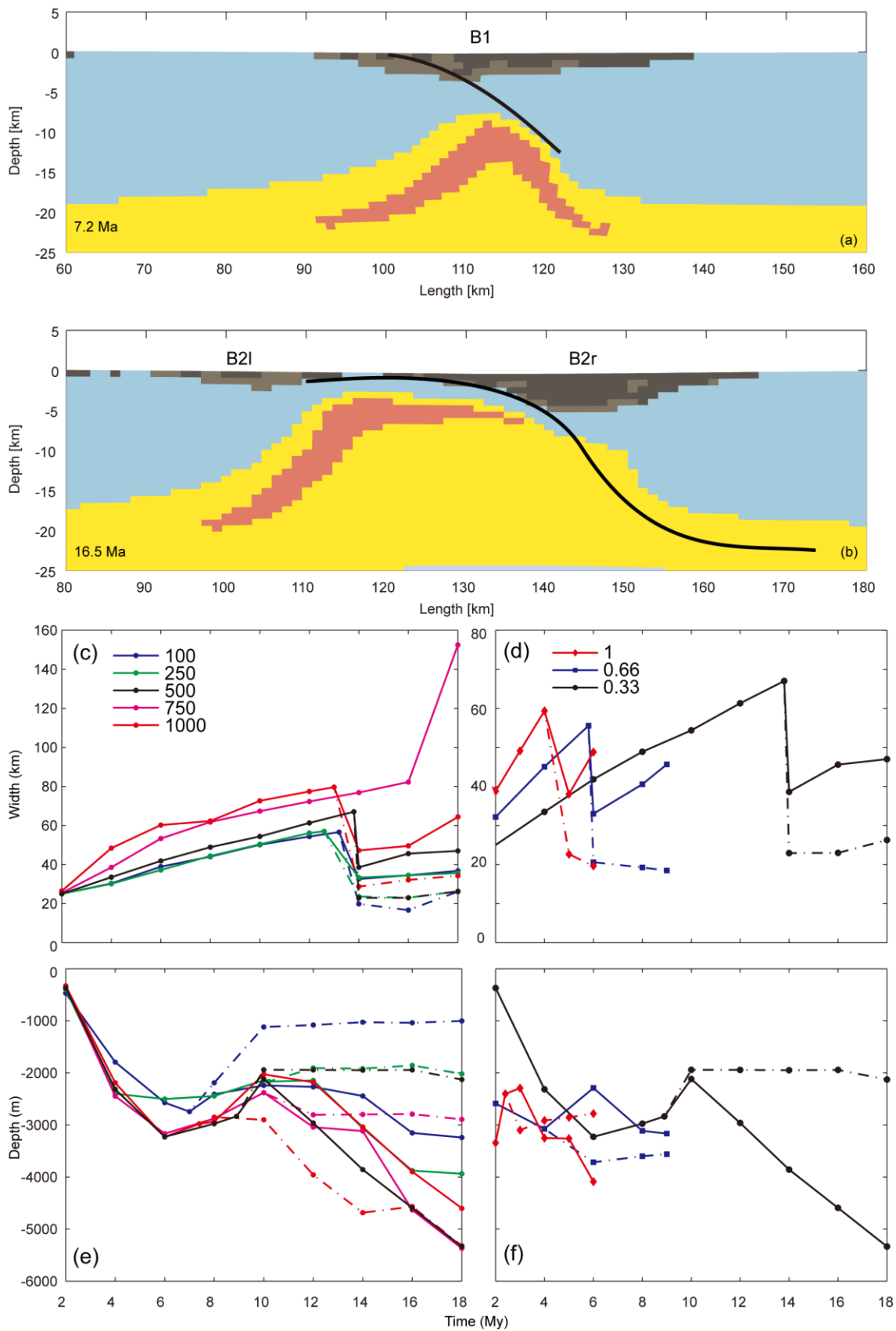
Figure 1

Figure 2

Figure 3

Figure 4

Figure 5

Figure 6

Figure 7

Figure 8

Pressure-Temperature paths of the passive markers
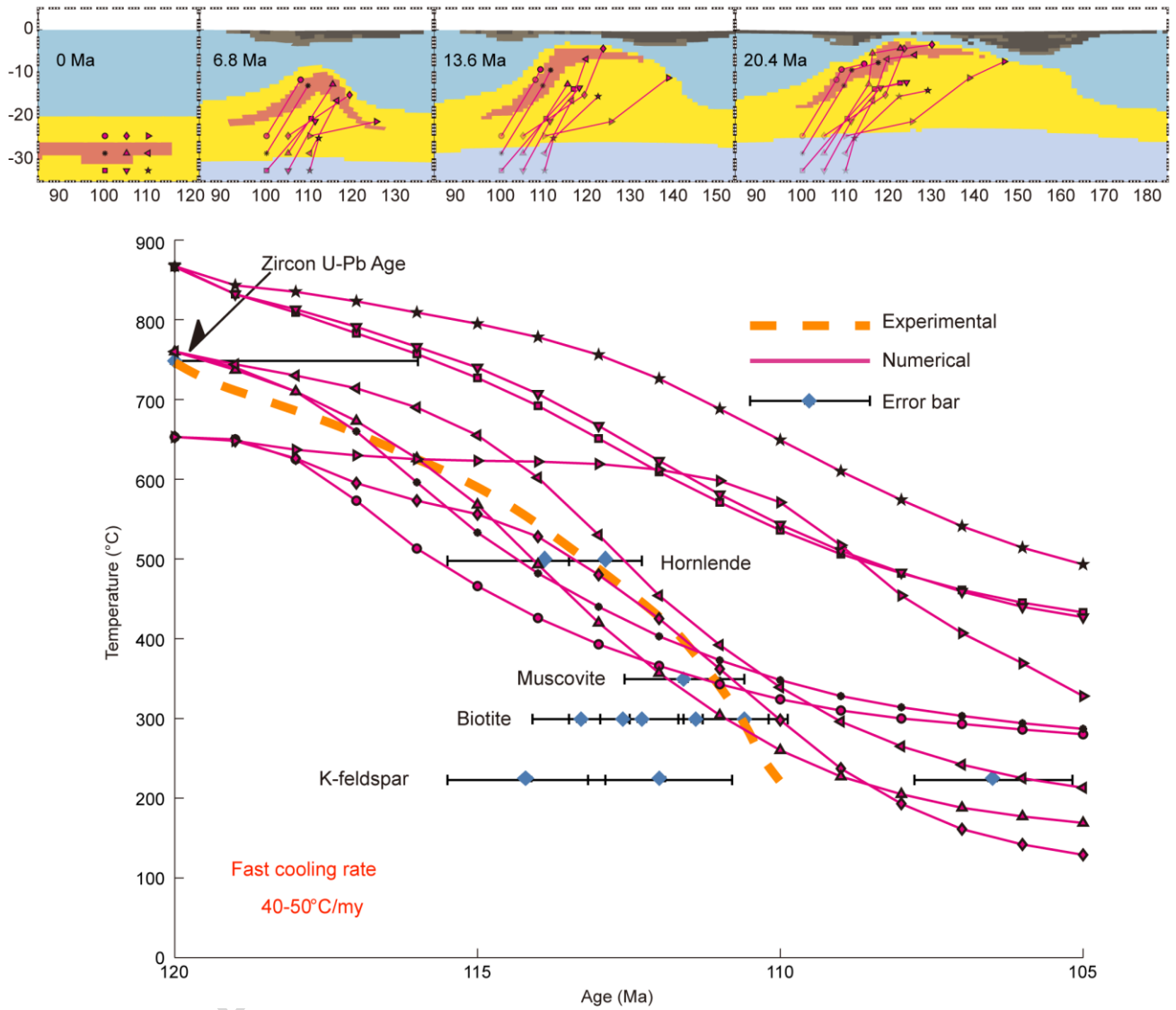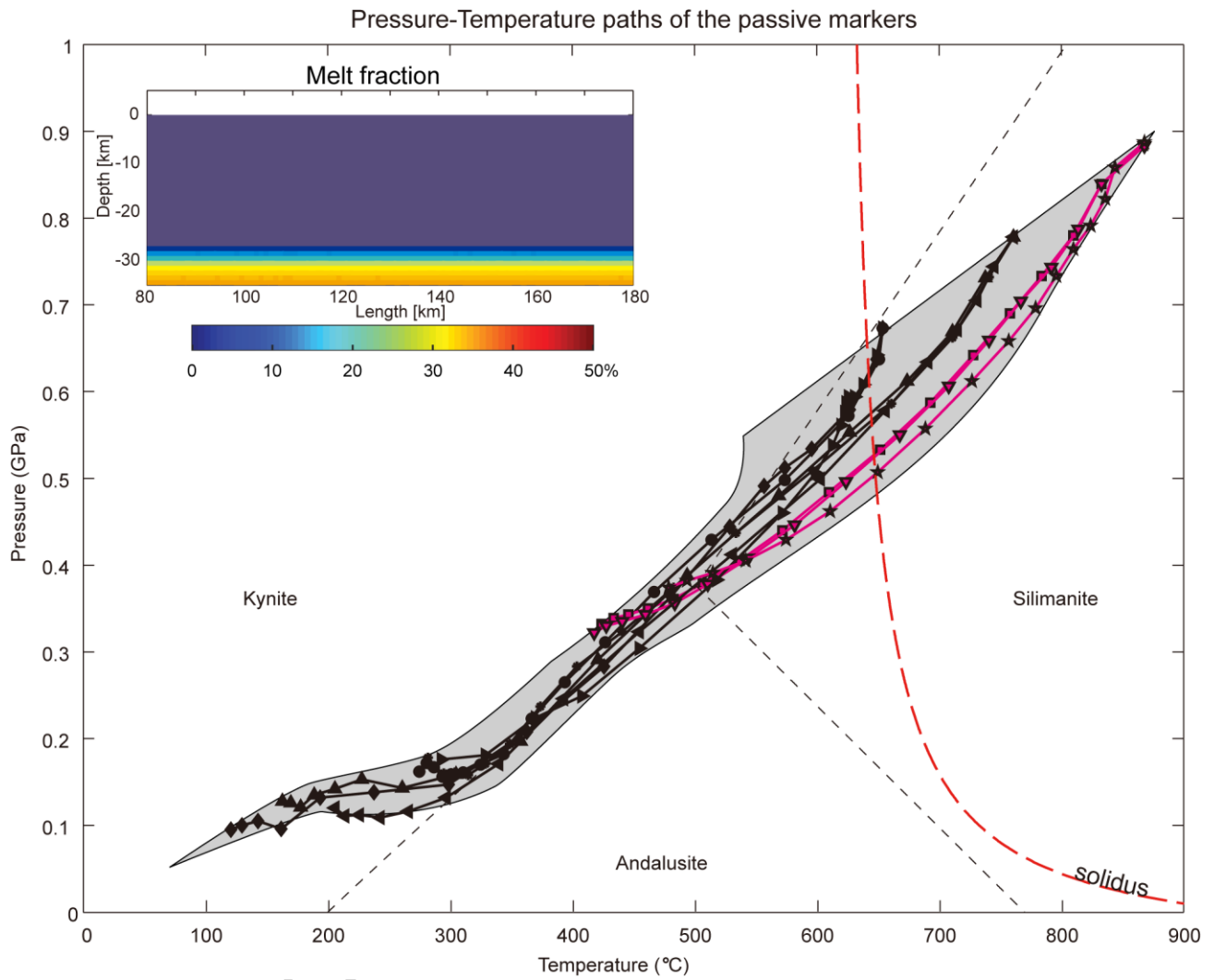
Highlights

Models of development of metamorphic core complex in normal continental crust.
Relationships between metamorphic core complexes and syn-rift basins.
Comparisons with observations in an atypical metamorphic core complex.